Journal of Marine Science and Application (2019) 18:482–491
https://doi.org/10.1007/s11804-019-00108-3

RESEARCH ARTICLE

Damage Detection in Reinforced Concrete Berthing Jetty Using a Plasticity Model Approach

Srinivasan Chandrasekaran[1] · P. T. Ajesh Kumar[1]

Received: 7 June 2018 / Accepted: 13 March 2019 / Published online: 6 November 2019

Abstract
A conventional method of damage modeling by a reduction in stiffness is insufficient to model the complex non-linear damage characteristics of concrete material accurately. In this research, the concrete damage plasticity constitutive model is used to develop the numerical model of a deck beam on a berthing jetty in the Abaqus finite element package. The model constitutes a solid section of 3D hexahedral brick elements for concrete material embedded with 2D quadrilateral surface elements as reinforcements. The model was validated against experimental results of a beam of comparable dimensions in a cited literature. The validated beam model is then used in a three-point load test configuration to demonstrate its applicability for preliminary numerical evaluation of damage detection strategy in marine concrete structural health monitoring. The natural frequency was identified to detect the presence of damage and mode shape curvature was found sensitive to the location of damage.

Keywords Structural health monitoring · Damage detection; natural frequency; Mode shape · Curvature · Damage parameters · Concrete damaged plasticity model · Finite element method · Numerical model

1 Introduction

Coastal structures like berthing jetties are concrete structures, which accumulate damage during their service life under the effect of environmental loads. These structural members are prone to faster deterioration due to continuous exposure to a highly corrosive environment. For example, in the Persian Gulf region, where the marine environment is characterized by hot-dry climate, desert features, and high salinity, longitudinal cracks and spalling were observed at different locations on the structure. It was particularly intense in areas where a patch repair was performed in the past. The poor quality and unsuitable components in concrete mix intensified corrosion rate and deterioration (Shekarchi et al. 2011). Also, the marine concrete structural members are infrequently subjected to accidental and seismic loads that cause damage to the concrete cover or result in crack formation.

The conventional assessment method for damage identification using manual inspection and non-destructive testing is hampered by poor visibility and hazardous conditions (Vandiver 1975). Visual and NDT-based inspections of such long jetties are costly and difficult to perform in remote locations of the structure. An instance of inspection of a facility shown in Fig. 1 shows the difficulty and risk associated with manual inspections. An instrument-based global structural health monitoring system using appropriate damage parameters can save many costs and serve multiple objectives ranging from primary assessment of the structural integrity to locating the position of the critical damage locations on the structure.

Structural health monitoring methods encompassing early detection of damage and estimation of structural integrity can be useful to initiate preventive maintenance; both cost and downtime during maintenance can be reduced considerably. Continuous or event-triggered structural health monitoring systems are also useful as proof of accident events and overloading on port and harbor structures (Srinivasan

Article Highlights
- In order for wave energy to be a viable energy option, the survivability in harsh offshore environments must be guaranteed.
- Peak forces in the connection line used in the wave energy concept developed at Uppsala University are studied.
- Three numerical models are presented and compared with each other and with the physical wave tank data.
- The performance of each model is studied and seen dependent on buoy geometry and applied level of power take-off damping.

✉ Srinivasan Chandrasekaran
drsekaran@iitm.ac.in

[1] Department of Ocean Engineering, Indian Institute of Technology Madras, Chennai, Tamil Nadu 600036, India

Fig. 1 Visual inspection at a colossal marine concrete structure

Chandrasekaran 2016). Choosing the right damage parameter for damage detection with better reliability estimates continues to be a challenge in this field. Damages in structural members lead to changes in physical properties, namely stiffness, damping, or mass of the structure, which may reflect as a change in modal frequencies and mode shapes. Changes in modal parameters, which reflect the damage level of the structure, can be traced through vibration measurements (Doebling et al. 1998). Changes in natural frequency of the structure, resulting from damaged members are good indices to detect, localize and quantify damages (Vandiver 1977; Gudmundson 1982). However, changes in natural frequency alone may not be sufficient for the unique identification of damage location (Salawu 1997). It is important to note that significant damage shall sometimes even result in an insignificant change in natural frequency (Salawu 1997).

The onset of damage and initial stages of progress does not make any significant and noticeable change in frequency, and it may be significantly influenced by the variation in the mass of structure and measurement noises (Zou et al. 2000; Ndambi et al. 2002; Kim et al. 2003). Mode shape, which is one of the vital inputs for damage detection, can highlight structural damages in higher modes; damages in higher modes are difficult to be captured by sensors used in vibration tests. Also, ambient noise and sensor positions largely affect the accuracy of damage detection based on a change in mode shapes (Kim et al. 2003). Mode shape curvature was studied for damage detection by several investigators. It was observed to be more effective than mode shapes in locating damage (Ismail et al. 2006, Rucevskis and Wesolowski 2010; Dawari and Vesmawala 2013; Vigneshwaran and Behera 2014; Ciambella and Vestroni 2015). The frequency-based and mode shape–based damage parameters were introduced to detect, localize, and quantify the damage from global vibration measurements. While the procedures for such damage detection are explicit in the literature, most of them are done for homogenous materials while the current study deals with heterogeneous material.

The present study focuses on developing a numerical model of an RC beam to generate damage response data and to use it to assess the performance of natural frequency, displacement mode shape, and mode shape curvature in damage detection of concrete structural members through a detailed analytical study. Damage parameters are selected based on their success in damage detection of homogenous materials, as reported in the existing literature. The present study explores the possibility of extending the application of frequency-based and mode shape–based damage parameters for damage detection in heterogeneous material, which has non-linear characteristics of material resistance. A reinforced concrete deck beam of a coastal berthing jetty is considered for the study.

2 Concrete Damaged Plasticity Model

Concrete is a heterogeneous quasi-brittle material with complex material characteristics. Its deformation characteristics change with type and magnitude of loading (Chi and Kirstein 1958; Hillerborg et al. 1976; Takahashi 1983; Buyukozturk and Tseng 1984; Buyukozturk and Shareef 1985). In a marine environment, corrosion of reinforcements is considered as one of the main causes of early deterioration of concrete. Corrosion leads to crack formation. The reliability of steel bar is time-dependent because corrosion leads to embrittlement of the steel and reduction in the number of cycles to fatigue failure (Apostolopoulos and Michalopoulos 2006). Structural characteristics and post-cracking behavior of concrete members are different during tension and compression. While the appearance of flexural cracks is primarily used to characterize the damage in concrete members; the actual structural integrity is influenced by the material properties and behavior of the member in tension and compression (Lubliner et al. 1989; Oller et al. 1990). Under low-magnitude pressure loads, concrete behaves in a brittle manner with failure mechanisms in the form of cracking in tension and crushing in compression. When the confining pressure is large enough to prevent crack propagation, the brittleness of concrete disappears. Under these conditions, material failure occurs by consolidation and collapse of the microporous microstructure in concrete resulting in characteristics that resemble a ductile material with work hardening (Lee and Fenves 1998). This varying complex non-linear behavior of concrete for different magnitudes of tension and compression and the resulting post-failure behavior is defined through damage plasticity model proposed by Lubliner et al. (1989) and modified later by Lee and Fenves (1998).

The model also takes into consideration the degradation of stiffness in concrete under the influence of damage. This constitutive model is based on the plasticity theory, developed

with appropriate allowance made for different values of parameters describing tension and compression. The response of concrete under higher loads can also be related to being similar to a frictional material with cohesion, with failure defined as complete loss of cohesion. In the model, the cohesion is defined through expression for yield criteria in plasticity theory–based damage models. A hardening rule is defined such that the total damage is assumed to correspond to the vanishing of cohesion.

The plasticity model used in this approach is a pressure-dependent model. The concrete damaged plasticity approach cannot be used to model concrete behavior under very large hydrostatic pressure. The concrete damaged plasticity model applies only for modeling concrete behavior under low confining pressure in the range of five times the ultimate compressive stress in uniaxial compression loading. The constitutive relations were derived based on these conditions using the yield criterion, flow rate, and the hardening rule (Lubliner et al. 1989; Lee and Fenves 1998). The CDP model uses a yield criterion based on the yield function proposed by Lubliner et al. The modifications proposed by Lee and Fenves are incorporated into it to account for the complex evolution of strength under tension and compression. The yield function is expressed in terms of the effective stresses as given below:

$$F\left(\bar{\sigma}, \tilde{\varepsilon}^{pl}\right) = \frac{1}{1-\alpha}\left(\bar{q} - 3\alpha p + \beta\left(\tilde{\varepsilon}^{pl}\right)\left\langle \hat{\bar{\sigma}}_{\max}\right\rangle - \left\langle -\hat{\bar{\sigma}}_{\max}\right\rangle\right) - \bar{\sigma}_c\left(\tilde{\varepsilon}_c^{pl}\right) \le 0 \quad (1)$$

where $p = -\frac{1}{3}\sigma \cdot I$ is the effective hydrostatic pressure; $q = \sqrt{\frac{3}{2}S \cdot S}$ is the Mises equivalent stress, $S = pI + \sigma$ is the deviatoric part of the effective stress tensor σ; and $\sigma_{\max}$ is the algebraically maximum eigenvalue of σ.

The function $\beta\left(\tilde{\varepsilon}^{pl}\right)$ is given as:

$$\beta(\tilde{\varepsilon}^{pl}) = \frac{\bar{\sigma}_c\left(\tilde{\varepsilon}_c^{pl}\right)}{\bar{\sigma}_t\left(\tilde{\varepsilon}_t^{pl}\right)}\,(1-\alpha) - (1+\alpha)$$

σ_t and σ_c are the effective tensile and compressive cohesion stresses, respectively.

The dimensionless material coefficient α can be determined from the initial equi-biaxial and uniaxial compressive yield stress, α_{b0} and α_{c0}, as:

$$\alpha = \frac{\sigma_{b0} - \sigma_{c0}}{2\sigma_{b0} - \sigma_{c0}}$$

Typical values of the ratio $\frac{\sigma_{b0}}{\sigma_{c0}}$ for concrete are in the range from 1.10 to 1.16, yielding values of α between 0.08 and 0.12 (Lubliner et al. 1989).

The dimensionless material coefficient γ enters the yield function only for stress states of tri-axial compression, when $\sigma_{\max} < 0$.

$$K_c = \frac{\gamma + 3}{2\gamma + 3}$$

The coefficient γ is evaluated as

$$\gamma = \frac{3(1-K_c)}{2K_c - 1}$$

A value of $K_c = \frac{2}{3}$ is typical of concrete, for which $\gamma = 3$.

The flow potential ϕ chosen for this model is the Drucker-Prager hyperbolic function:

$$\phi = \sqrt{(\varepsilon\sigma_{t0}\tan\psi)^2 + q^2} - p\tan\psi$$

where ψ the dilation angle is measured in the p–q plane at high confining pressure; σ_{t0} is the uniaxial tensile stress at failure; and ε is a parameter, referred to as the eccentricity that defines the rate at which the flow potential approaches to a straight line as the eccentricity tends to zero. This flow potential, which is continuous and smooth, ensures that the flow direction is defined uniquely. Plastic flow is non-associated. Since the model uses non-associated plasticity, it requires the solution of non-symmetric equations. Some of the convergence difficulties during an implicit analysis of material models that exhibit softening behavior and stiffness degradation in the implicit analysis in ABAQUS can be overcome by using a visco-plastic regularization of the constitutive equations. A viscosity parameter μ represents the relaxation time of the visco-plastic system. Using the visco-plastic regularization and a smaller value for the viscosity parameter compared with the characteristic time increment improves the rate of convergence of the model in the softening regime, without compromising the results (ABAQUS 2013).

3 Methodology

The present numerical study using a finite element model of reinforced cement concrete beam involved the following stages. The first stage is numerical modeling of the RC beam in ABAQUS finite element package in a four-point load test configuration. It enables the simulated model to be evaluated against existing experimental data in the literature. The second stage involved inducing damage in the damage plasticity model of RC beam and computing the frequency and modal parameters of the beam with varying levels of damage progress. A three-point load test configuration is used to induce damage in structure through a loading and unloading procedure. An eigenvalue extraction method in ABAQUS linear perturbation frequency analysis module was used after to extract natural frequencies and mode shapes. In the third stage, the damage

response data is used to compute the damage parameters using MATLAB and interpret the results.

The first stage in this study is the development of a numerical model of the RC beam in ABAQUS finite element package. The model is developed in a four-point load test scheme and verified by comparing its static and modal response with existing results in the literature. In the next stage, the developed and verified model is applied for the study, as an example problem. The damage was induced in the model by loading and unloading, at specific load magnitudes. The load magnitudes were chosen as 40, 60, 80, and 104 kN. These damage cases in increasing order of severity were named as D40kN, D60kN, D80kN, and D104kN, respectively. Mid-span deflection before and after damage and the changes in natural frequency due to damage and as well as from changes in topside mass are recorded and compared. Several SHM systems interpret the presence of damage from changes in natural frequency. However, in this research, the accuracy of the damage detection using natural frequency under the influence of changes in topside weight at the deck of a reinforced concrete berthing jetty due to loading and unloading activities is examined. The topside was loaded with point masses of 100 kN and 160 kN to generate two test cases of variation in topside weight of the structure during the operational period.

In this study, the midspan deflection of the beam is used to represent damage severity. The damage severity index based on mid-span deflection is defined as:

$$\mathrm{DI} = 1 - \frac{\delta_0}{\delta}$$

where δ_0 and δ are mid-span deflection for the undamaged and damaged beam for a given load case (Perera et al. 2008). When progressive material degradation occurs in reinforced concrete, in addition to plastic deformation, the stiffness of the material also gets reduced. The deflection of a beam at mid-span is inversely related to its stiffness. Hence, for a given load, the deflection of the damaged beam is larger than that of the undamaged beam. When material degradation occurs in concrete due to damage, the stiffness gets reduced. The deflection of a beam at mid-span is inversely related to its stiffness. Hence, for a given load, the deflection of the damaged beam is larger than that of the undamaged beam. However, the rate of the change in deflection with increasing load reduces in the plastic region compared with that in the undamaged linear region. The lower slope would mean that the subsequent values of deflection will be closer in the plastic region for an equal amount of increase in load. The damage severity index for an undamaged beam under its self-weight is zero. When the static load is increased in steps of equal increments, the damage severity increases in uniform proportion in the linear response region. When the response enters the plastic region, the DI values are squeezed together with no uniformity in a change in DI for uniformly increasing the load.

The dependency between deflection of the beam and change in natural frequency change under the influence of damage makes it an important parameter for damage assessment (Gillich et al. 2012). The difference in the natural frequencies of the damaged and undamaged beam can be indicative of the presence of damage. Higher frequency shift means more severity of the damage. The damage parameter based on a change in natural frequency is defined as:

$$\Delta f = f_u - f_d$$

where f_u is the frequency for the undamaged state and f_d is for the damaged ones.

The presence of damage can cause a change in the magnitude of mode shape. Mode shape curvature, the second derivative of mode shape, is related to bending moment by the equation

$$\kappa = \frac{M}{EI}$$

where EI is flexural rigidity, M is the bending moment, and κ is the mode shape curvature at a given location.

4 Finite Element Model

The RC beam model used for the current study is a scaled down model of an 18-m concrete beam of a berthing jetty structure, retaining the aspect ratio. The model was scaled down to a length of 4.54 m, enabling verification of the numerical model for its performance and accuracy with existing results about a beam of comparable dimensions reported in the literature. A four-point load test arrangement was developed as a finite element model in ABAQUS software with loading and boundary conditions as shown in Fig. 2.

The cross-section of the RC beam in Fig. 3 shows the dimensions and distribution of reinforcements. The RC beam model consists of a solid beam with rebar embedded into it as shell elements. The solid beam is defined as a homogenous solid section and assigned a mesh with eight-node linear brick element C3D8. In order to model reinforcements, the "embedded elements" technique in the "constraints" module of ABAQUS was used. In this technique, an element or group of elements is embedded in "host" elements. It can be used to model rebar or reinforcement. If a node of an embedded element lies within a host element, the translational degrees of freedom at the node are eliminated, and the node becomes an "embedded node." The translational degrees of freedom of the embedded node is constrained to the interpolated values of the corresponding degrees of freedom of the host element. In the present model, a surface layer is created in the concrete solid

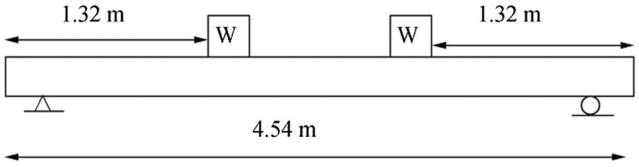

Fig. 2 Schematic diagram of the beam in four-point load test arrangement

model, and a shell element is embedded at this surface layer. The embedded element defined as a shell element is embedded in solid using a four-node linear quadrilateral surface element SFM3D4. The beam reinforcements consist of 2 bars of 6-mm diameter running longitudinally over compression side, 4 bars of 12-mm diameter running longitudinally over tension side, and shear rebar stirrups of 6-mm diameter running transversely at every 200 m along the length of the beam. Two load points were created at 0.86 m from the middle. Two supports were provided at 0.09 m from the beam ends.

Two material properties were created, steel and concrete. Steel rebar material is configured as deformation plasticity material with Young's modulus 210GPa, Poisson's ratio 0.3, and density 7850 kg/m^3. Concrete density is set at 2300 kg/m^3. Young's modulus of the concrete is set at 34 GPa and Poisson's ratio is set at 0.2. A 50-MPa high-strength concrete is considered for the study. For the non-linear region of the material characteristics, concrete damaged plasticity features were adopted from a validated model of reinforced concrete (Srinivasan and Ajesh, 2014). The material input to the model to generate the complex non-linear characteristics in compression and tension is shown in Figs. 4 and 5.

The four-point load test model of the RC beam in ABAQUS after assembly is shown in Fig. 6. The boundary conditions at the bottom include fixed support and roller support. The natural frequency computed from the numerical model of the beam with rigid support is 27.647 Hz. In order to correlate the model with the experimental setup, the rigid supports at the bottom were replaced by spring elements. At the bottom region of the beam, the "engineering features" option in "assembly module" is used to assign six springs as supports connected to the ground, each with spring constant of 0.8e7N/m. The spring stiffness is chosen through a series of repeated numerical evaluation to make the natural frequency of the numerical model to be close to a value of 25.32 Hz of the experimental specimen of Perera et al. (2008). In this study, since the change in frequency of the model with rigid support and spring support is very small, the rigid support model was used for the damage simulation study after validation of the model.

The coordinate axes were chosen as X along the length of the beam, Y along the depth, and the Z-axis along the width of the beam. The beam is fixed from movement in X and Z direction at the bottom. In the experimental analysis, the beam vibrations are measured in the Y direction with hammer excitation in the Y direction. In order to simulate the model behavior closer to that of the experimental ones, the vibration of the body in the Z direction is restricted by declaring fixed boundary conditions at one of the vertical faces on the side. The instances were created as an independent instance, and hence, the meshing was done for the entire assembly. Mesh quality was checked to see if corner angles are less than 45° or greater than 135°. Element size was optimized and chosen as 0.009 for accuracy and optimum computational load.

5 Model Validation

The natural frequency of the beam model with rigid support is 27.647 Hz, and with spring support is 25.3 Hz, which is comparable to the 25.32-Hz natural frequency of the beam in the experimental setup by Perera et al. (2008). In addition to the natural frequency, the first and second mode shapes and mid-span deflection were considered as the parameters for model verification. The first mode shape and second mode shape were generated in the "eigenvalue extraction method" of "linear perturbation module" of Abaqus. Mid-span deflection was considered for increasing magnitude of point load applied on

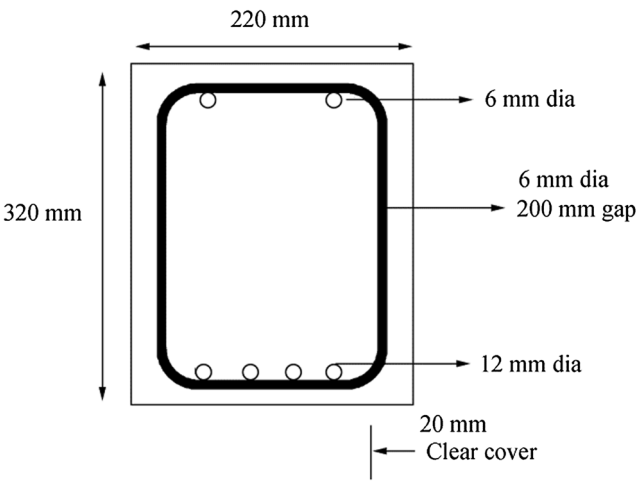

Fig. 3 Beam cross-section with reinforcement distribution

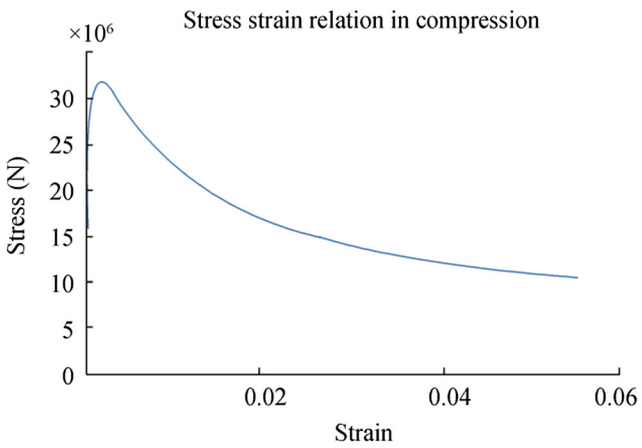

Fig. 4 Complex non-linear characteristics of concrete in compression

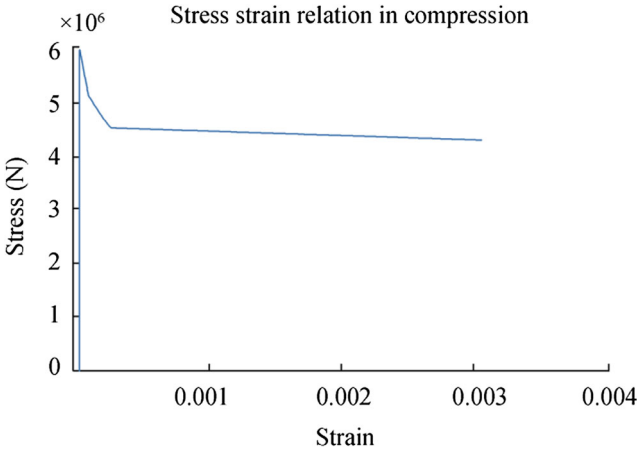

Fig. 5 Complex non-linear characteristics of concrete in tension

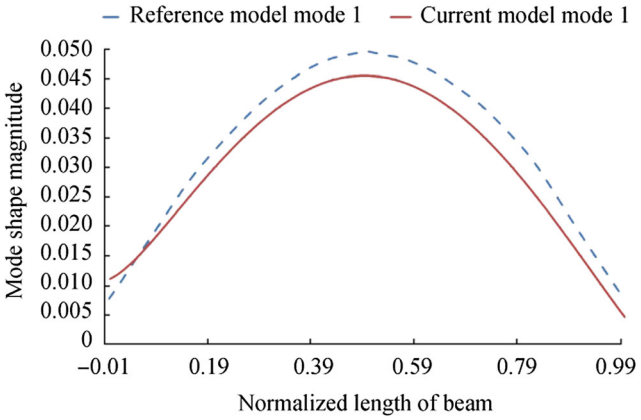

Fig. 7 Mode shapes of the current model and the reference model at mode 1

the structure. The results were compared with existing results for a comparable structural member (Perera et al. 2008).

In Fig. 7, the mode shapes of the beam model and its reference model at first mode are compared. In Fig. 8, the mode shapes of the beam model and the reference model for the second mode are compared. In Fig. 9, the mid-span deflection of the model is compared with the reference model. The pattern observed in responses of the static test as well as the modal test matches with that of the reference model. The deviation of the current model from the values reported in the literature is less than 10%, and hence, the model is validated for static deflection as well as for mode shapes.

6 Damage Detection Studies

The RC beam model evaluated in ABAQUS was used for further investigation in damage detection studies. In order to generate modal parameters under undamaged and damaged conditions, the RC beam model was configured to match the experimental setup of a three-point load test arrangement, retaining the fundamental dimensions of the previous study.

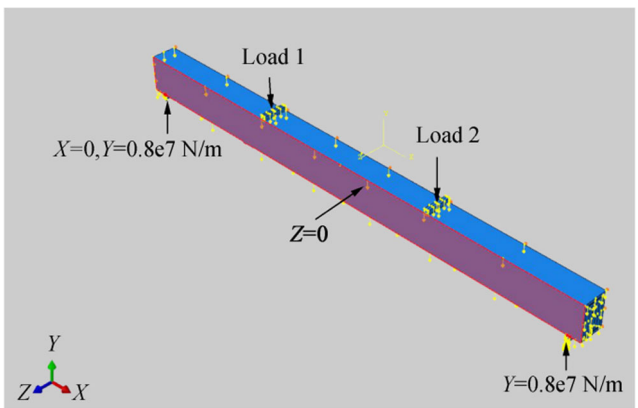

Fig. 6 RC beam model after assembly in ABAQUS

In the current study, the damage is generated at the mid-span by fixing the load point at the center of the beam. Damage in the beam is introduced by loading and unloading at the load point, as shown in Fig. 10. To simulate different levels of damage severity, seven static load cases were considered which are 8, 20, 40, 52, 60, 80, and 104 kN. Among these seven load cases, 2 cases are for undamaged conditions and the rest of 5 cases are for damaged conditions. The load 40 kN indicates the onset of damage and the load 104 kN represents extreme damage. The presence of residual strain in the RC beam after every unloading step is also clear from the load v/s mid-span deflection plot shown in Fig. 11. The magnitude of the residual deflection for ascending order of load magnitudes increased after every cycle of loading and unloading. It indicates that during each loading and unloading cycle, the material has acquired damage in it. It is also observed that the crack generation in the RC beam begins when the load reaches 40 kN. For all the load cases above 40 kN, when the load is increased, the deflection is non-linear. In all such cases, after unloading, it leaves a residual strain with deflection not returning to its initial position.

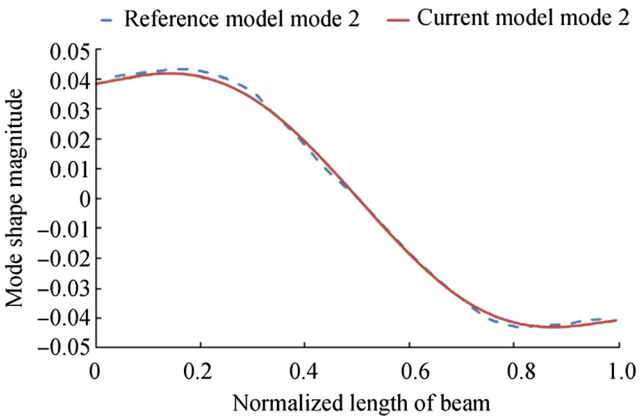

Fig. 8 Mode shapes of the current model and the reference model at mode 2

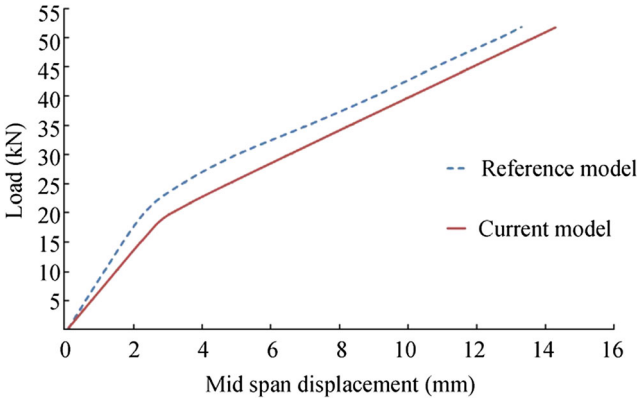

Fig. 9 Mid-span deflection of the current model and the reference model

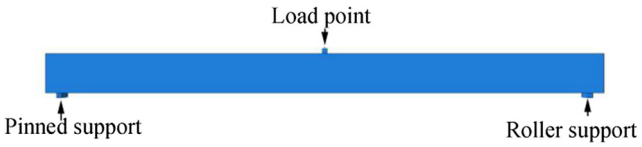

Fig. 10 Three-point load test configuration for damage detection studies

In the concrete damaged plasticity model in ABAQUS, it is not possible to visualize the crack as it is. The damage occurs in areas where the strain is localized. The effect of crack generation or its propagation results in a change in strain field around the crack location. In ABAQUS, it is assumed that cracking begins at points where the tensile equivalent plastic strain is greater than zero and the maximum principal plastic strain becomes positive (ABAQUS 2013). The direction of the vector normal to the crack plane is assumed to be parallel to the direction of the maximum principal plastic strain. This direction can be viewed in the visualization module of ABAQUS using the symbol plot of maximum principal plastic strain tensor PE at integration points of the finite element model. Figure 12 shows the symbol output of the maximum principal plastic strain tensor PE at integration points.

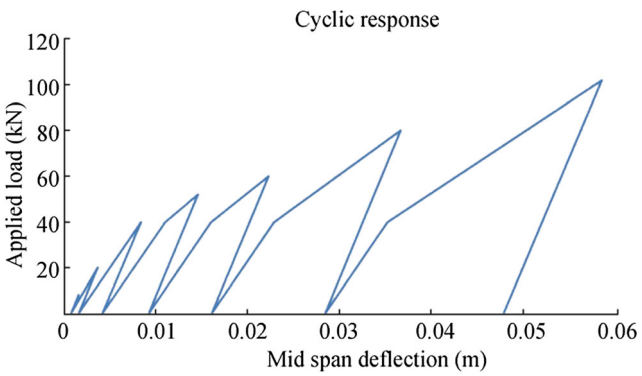

Fig. 11 Response to cyclic load with increasing magnitude

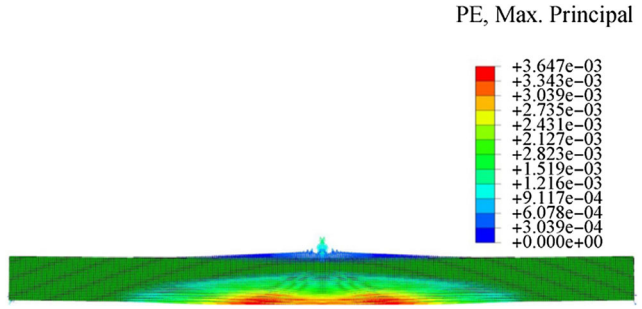

Fig. 12 Severity of damage represented using the symbol plot of maximum principal strain PE

7 Results and Discussions

The damage detection study involved static and dynamic analysis. After each unloading step, a linear perturbation analysis was done to extract natural frequencies and mode shapes. The pre-damage and post-damage deflection of the RC beam was compared to understand the influence of damage on a deflection of the beam. Figure 13 shows the deflections of the beam before and after the damage is induced at mid-span. The peak values of the deflection at mid-span are shown in Table 1. The deflection is recorded for three conditions. The first one is when the beam is in baseline condition with no damage at all. When the 104-kN load is applied, the beam deflects, and it also develops a crack. However, the deflection at this load happened when the beam was undamaged. The second deflection is recorded after unloading the beam. Since the beam is now damaged, there will be a residual deflection. The third deflection is recorded by loading the beam with residual deflection, which is the damaged case. Since the damage has caused a reduction in strength of the beam, the deflection is observed to be higher than the first load case. It is observed that deflection of the beam due to 104-kN load generates crack and damages the beam such that even after removal of the load, the beam does not return to its initial position. There is a residual deflection in the beam, indicating that it has entered the plastic region. For a load of 104 kN applied again to the damaged beam, the beam deflection is observed to be higher

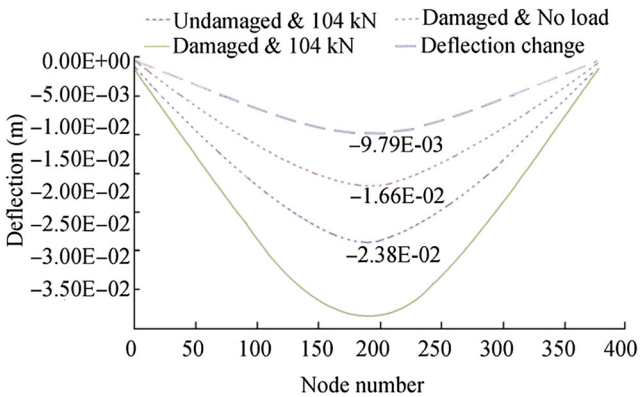

Fig. 13 Mid-span deflection of the damaged and undamaged beam

Table 1 Comparison of peak deflections at mid-span

Damage case	Maximum deflection
104-kN load on the undamaged beam	2.36e-2
Beam unloaded (damaged)	1.66e-2
104-kN load on the damaged beam	3.36e-2

than that of the undamaged beam. It indicates that in addition to plasticity, the beam has also lost some of its stiffness. The numerical model represents both the plasticity effects as well as the reduction in stiffness under damage conditions.

Computation of damage parameters is performed for seven levels of damage severity. These levels correspond to 8, 20, 40, 52, 60, 80, and 104 kN. The first two levels, 8 kN and 20 kN, are undamaged conditions. Hence, 8 kN is set as a reference level of undamaged and 20 kN is used to depict the transition from undamaged to the onset of damage at 40 kN. The damage severity index is computed for each of the damage levels using mid-span deflection data. The natural frequency is plotted for various damage severities in Fig. 14. The natural frequency is found to be different for damaged and undamaged cases. The change in the natural frequency is observed to be higher in mode 2. Table 2 shows a change in natural frequency of the beam for increasing damage severity in mode 1 and mode 2. It is observed that at mode 1 and mode 2, the change in natural frequency increases with an increase in the damage severity. The change in the natural frequency at first mode is found to be very small to be applied for damage detection. However, the change in natural frequency increased at the second mode, indicating that at higher modes, natural frequencies have a higher sensitivity to damage. The change in natural frequency may be an indication of the presence of damage, but it cannot be ascertained without a further detailed investigation. For example, a change in mass during operations can also cause a change in the natural frequency. Also, accurate measurement of higher frequencies is practically difficult due to sensor limitations. Hence, natural frequency

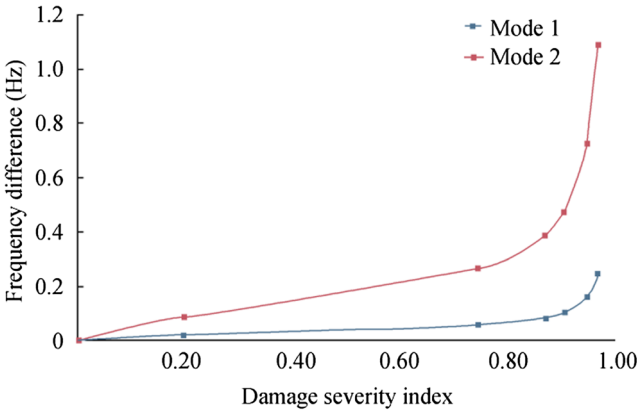

Fig. 14 Change in natural frequency for increasing damage severity calculated using Eq. (1)

Table 2 Change in natural frequency at mode 1 and mode 2 for increasing damage severity DI calculated from deflections using Eq. (1)

Damage case	Damage severity	Mode 1, freq change (Hz)	Mode 2, freq change (Hz)
D8kN	0	0	0
D20kN	0.19	0.02	0.09
D40kN	0.74	0.05	0.27
D52kN	0.87	0.08	0.39
D60kN	0.90	0.10	0.47
D80kN	0.95	0.16	0.73
D104kN	0.97	0.25	1.09

measured using the existing technologies is not a reliable damage parameter to detect and locate damages.

Figures 15 and 16 show a comparison between the magnitude of the mode shape for the undamaged case and damaged cases at both the first and second modes, respectively. The difference in magnitude of mode shapes for damaged and undamaged cases is very low that it cannot be used for damage detection accurately. However, the damage detection property improves when the mode shape curvature is computed from the mode shape data and plotted using MATLAB software.

Figures 17 and 18 show the mode shape curvature for undamaged beam and damage in the beam at mid-span for both the first and second modes, respectively. A zoomed view of the mode shape curvature response at mid-span region for the second mode has been generated in Fig. 19. It is observed that mode shape curvature changes significantly in the damage region as compared to the rest of the undamaged region. In the zoomed view, it is also observed that for varying damage severity, there is a clear distinction in the magnitude of mode shape curvature. The response of mode shape curvature increased in magnitude for higher magnitude. It indicates that mode shape curvature can effectively detect the presence of

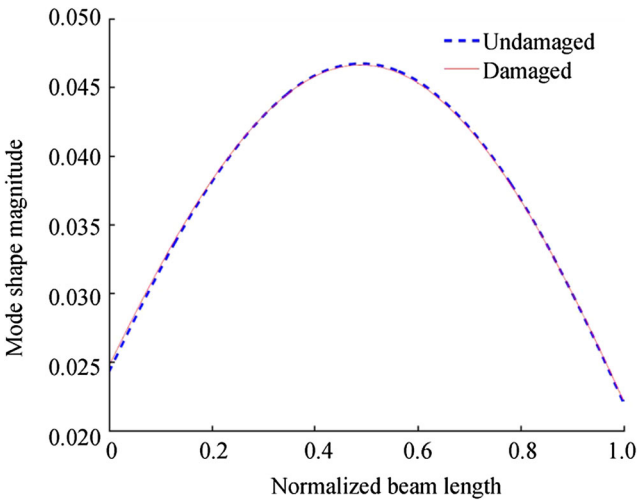

Fig. 15 Mode shape of the undamaged and damaged beam at mode 1

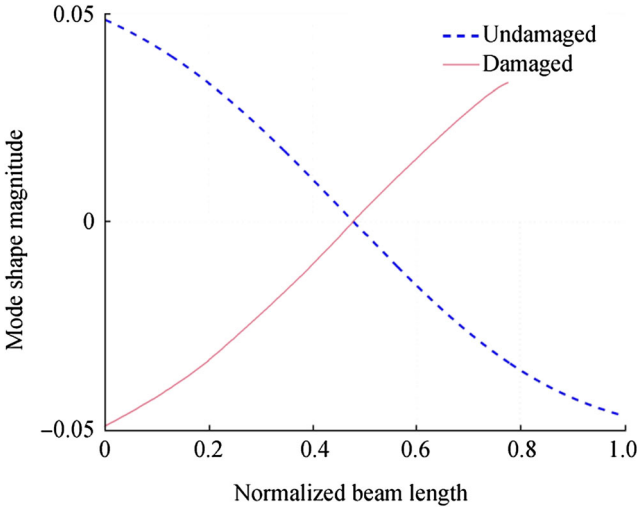

Fig. 16 Mode shape of the undamaged and damaged beam at mode 2

damage and also locate it, even without the baseline data of the beam. The damage progress in the beam can be detected by periodically generating mode shape curvature response and comparing the perturbations in the plot with the regions of the plot that are close to zero. The increased magnitude in the certain region indicates that that region is damaged compared with the region with response around zero lines.

8 Conclusions

A detailed analytical study is conducted about frequency-based and mode-based damage detection methods applied to RC beam in coastal structure. The study demonstrated the feasibility of using the concrete damaged plasticity constitutive model to simulate the complex non-linear damage characteristics of reinforced concrete members. The validated damage model was used in a three-point load test

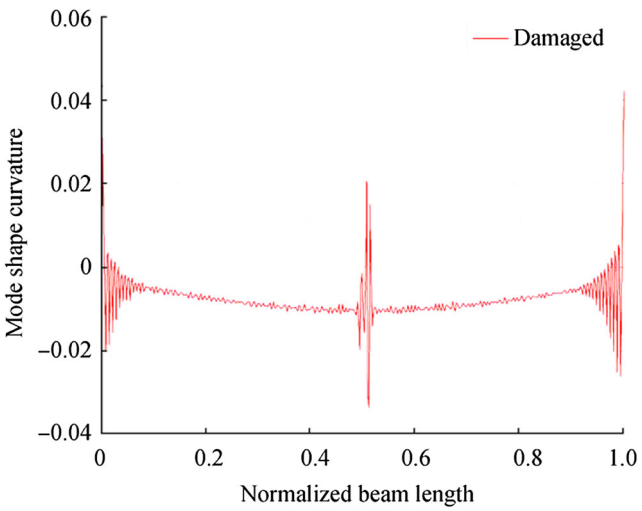

Fig. 17 Mode shape curvature of the undamaged and damaged beam at mode 1

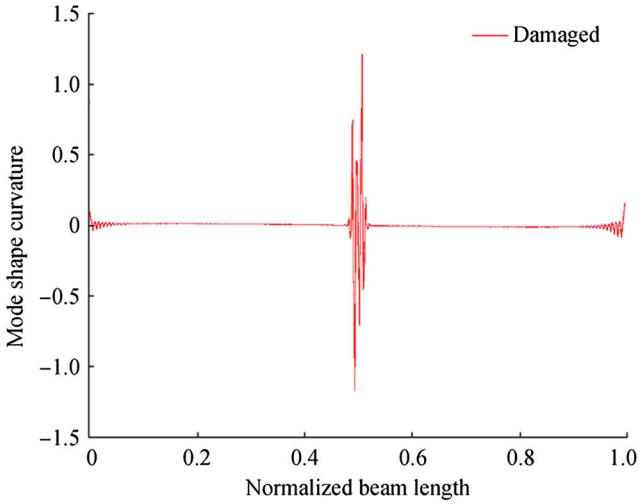

Fig. 18 Mode shape curvature of the undamaged and damaged beam at mode 2

configuration to study the sensitivity of various damage parameters to the severity of damage. It is observed that natural frequency effectively detects the presence of damage at higher modes, but it fails to identify the location of damage. The change in mode shape of the damaged beam is very low to distinguish it from that of the undamaged beam. However, the mode shape curvature derived from mode shape successfully detects and locates damage for the mid-span damage case. However, the effectiveness and accuracy of damage detection using mode shape curvature need to investigated for multiple crack cases and cracks in different locations on the beam. The accuracy of damage detection can be achieved if the resolution of sensor position is higher enough to capture all the information. In general, the more the number of sensors is used, the more detailed information of the structure can be obtained. However, it increases the number of devices and the

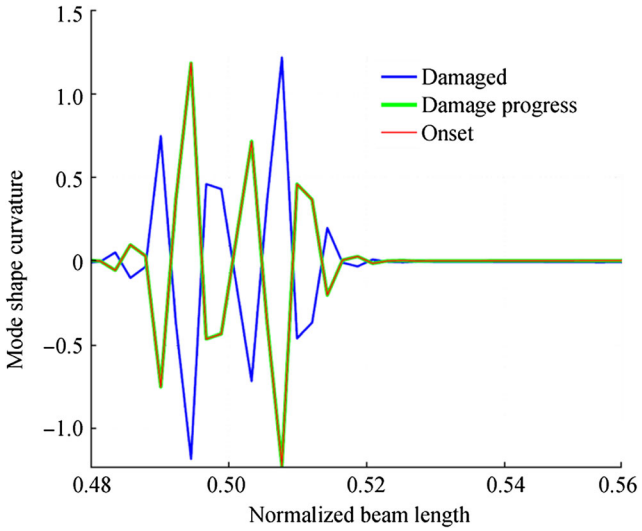

Fig. 19 Zoomed view of the mid-span region comparing mode shape curvature of the undamaged and damaged beam at mode 2

associated workloads. Hence, the number of sensors and the position of sensors need to be optimized based on multi-criteria sensor optimization techniques. Such optimization methods used information based on prior knowledge of the structure and finite element analysis. Hence, the current study is an essential tool to determine the possible locations of damage on a beam and add information to sensor optimization algorithms.

References

ABAQUS (2013) Abaqus Analysis User Manual - Abaqus Version 6.13. Available from http://50.16.176.52/v6.13/books/stm/default.php

Apostolopoulos CA, Michalopoulos D (2006) Effect of corrosion on mass loss, and high and low cycle fatigue of reinforcing steel. J Mater Eng Perform 15(6):742–749. https://doi.org/10.1361/105994906X1

Buyukozturk O, Shareef SS (1985) Constitutive modeling of concrete in finite element analysis. Comput Struct 21(3):581–610. https://doi.org/10.1016/0045-7949(85)90135-x

Buyukozturk O, Tseng TM (1984) Concrete in biaxial cyclic compression. J Struct Eng 110(3):461–476. https://doi.org/10.1061/(asce)0733-9445(1984)110:3(461)

Chandrasekaran S (2016) Offshore structural engineering: reliability and risk assessment. CRC Press

Chandrasekaran S, Ajesh Kumar PT (2014) Characterizing structural degradation with crack depth in RC beam of coastal jetty: numerical studies. Proc. of the ninth Structural Engineering Convention (SEC), Delhi, India

Chi M, Kirstein AF (1958) Flexural cracks in reinforced concrete beams. J Am Concrete Inst 54(10):865–878

Ciambella J, Vestroni F (2015) The use of modal curvatures for damage localization in beam-type structures. J Sound Vib 340:126–137. https://doi.org/10.1016/j.jsv.2014.11.037

Dawari VB, Vesmawala GR (2013) Structural damage identification using modal curvature differences. IOSR J Mech Civ Eng 4:33–38

Doebling SW, Farrar CR, Prime MB, Shevitz DW (1998) Damage identification and health monitoring of structural and mechanical systems from changes in their vibration characteristics: a literature review. Los Alamos National Laboratory report, LA-13070-MS. https://doi.org/10.2172/249299

Gillich GR, Praisach ZI, Negru I (2012) The relationship between changes of deflection and natural frequencies of damaged beams. Advances in Remote Sensing, Finite Differences and Information Security: (F-And-B 012), (REMOTE 012), (ISP 012), WI, 38-42

Gudmundson P (1982) Eigen frequency changes of structures due to crack, notches or their geometrical changes. J Mech Phys Solids 30(5):339–353. https://doi.org/10.1016/0022-5096(82)90004-7

Hillerborg A, Modéer M, Petersson PE (1976) Analysis of crack formation and crack growth in concrete using fracture mechanics and finite elements. Cem Concr Res 6(6):773–781. https://doi.org/10.1016/0008-8846(76)90007-7

Ismail, Z., H. A. Razak, and A. A. Rahman (2006). Determination of damage location in rc beams using mode shape derivatives. Engineering Structures, 28(11):1566–1573.

Kim JT, Ryu YS, Cho HM, Stubbs N (2003) Damage identification in beam-type structures: frequency-based method v/s mode-shape-based method. Eng Struct 25:55–67. https://doi.org/10.1016/S0141-0296(02)00118-9

Lee J, Fenves GL (1998) Plastic-damage model for cyclic loading of concrete structures. J Eng Mech 124(8):892–900. https://doi.org/10.1061/(ASCE)0733-9399(1998)124:8(892)

Lubliner J, Oliver J, Oller S, Onate E (1989) A plastic-damage model for concrete. Int J Solids Struct 25(3):299–326. https://doi.org/10.1016/0020-7683(89)90050-4

Ndambi JM, Vantomme J, Harri K (2002) Damage assessment in reinforced concrete beams using eigenfrequencies and mode shape derivatives. Eng Struct 24:501–515. https://doi.org/10.1016/S0141-0296(01)00117-1

Oller S, Onate E, Oliver J, Lubliner J (1990) Finite element nonlinear analysis of concrete structures using a “plastic-damage model”. Eng Fract Mech 35(1–3):219–231. https://doi.org/10.1016/0013-7944(90)90200-Z

Perera R, Huerta C, Orquin JM (2008) Identification of damage in RC beams using indexes based on local modal stiffness. Constr Build Mater 22:1665–1667. https://doi.org/10.1016/j.conbuildmat.2007.06.012

Rucevskis S, Wesolowski M (2010) Identification of damage in a beam structure by using mode shape curvature squares. J Sound Vib 17:601–610. https://doi.org/10.3233/SAV-2010-0551

Salawu OS (1997) Detection of structural damage through changes in frequency: a review. Eng Struct 19(9):718–723. https://doi.org/10.1016/S0141-0296(96)00149-6

Shekarchi M, Moradimarani F, Pargar F (2011) Corrosion damage of a reinforced concrete jetty structure in the Persian Gulf: a case study. Struct Infrastruct E 7(9):701–713. https://doi.org/10.1080/15732470902823903

Takahashi Y (1983) Elastic-plastic constitutive modeling of concrete, No. ANL-83-23. Argonne National Lab

Vandiver JK (1975) Detection of structural failure on fixed platforms by measurement of dynamic response. Offshore Technology Conference. https://doi.org/10.4043/2267-MS

Vandiver JK (1977) Detection of structural failures on fixed platforms by measurement of dynamic response. J Pet Technol 29(3):305–310. https://doi.org/10.2118/5679-PA

Vigneshwaran K, Behera R (2014) Vibration analysis of a simply supported beam with multiple breathing cracks. Procedia Eng 86:835–842. https://doi.org/10.1016/j.proeng.2014.11.104

Zou Y, Tong L, Steven GP (2000) Vibration-based model dependent damage (delamination) identification and health monitoring for composite structures - a review. J Sound Vib 230(2):357–378. https://doi.org/10.1006/jsvi.1999.2624